7. Fluoreszenz-Resonanz-Energie-Transfer (FRET)

FRET ist eine wichtige Methode zur Untersuchung der Konformationsverteilung und der Dynamik von biologischen Molekülen.

7.1 Mechanismus des Energietransfers (*T. Förster 1948*)

Energieübertragung von angeregten Fluorophormolekülen eines DONORS auf relativ weit entfernte (1...8 nm) Fluorophormoleküle eines AKZEPTORS im Grundzustand. Wesentlich ist die Überlappung des FLuoreszenzspektrums des Donors mit dem Absorptionsspektrum des Akzeptors.

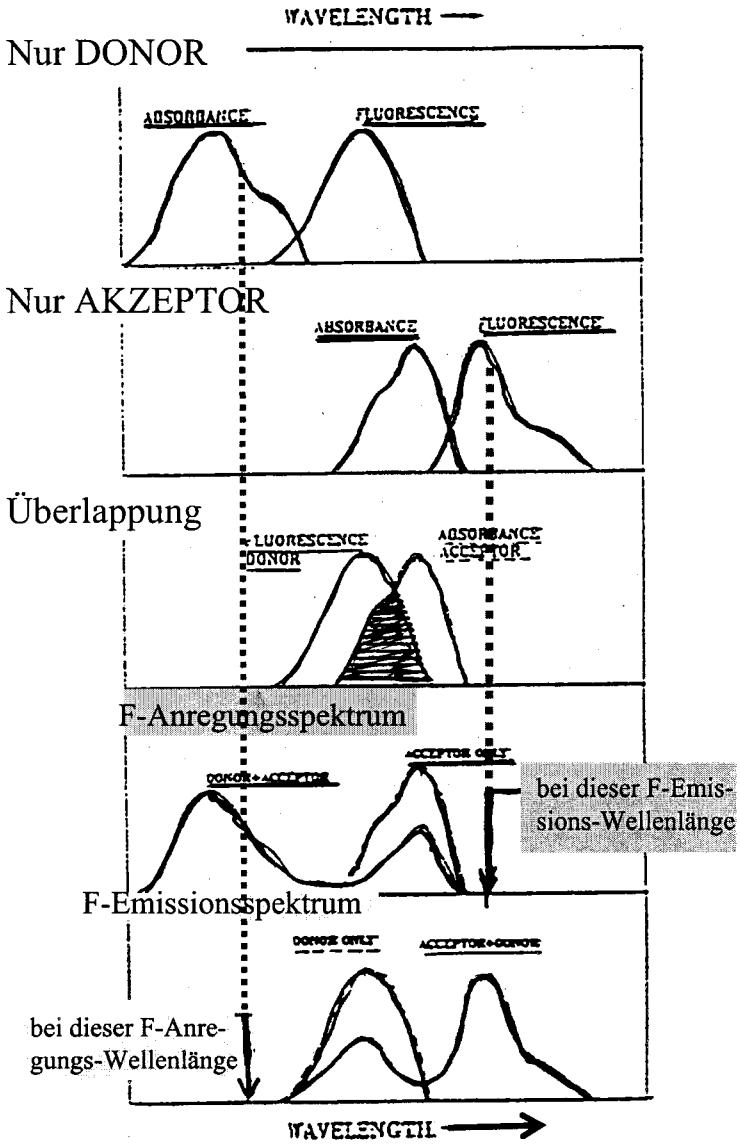

Nach *Förster* erfolgt der Energietransfer über die Dipol-Dipol-Wechselwirkung der Donor-Fluoreszenz-Dipole mit den Akzeptor-Absorptions-Dipolen.

→ Donor

$$\frac{1}{\tau} = \frac{1}{\tau_0} + k_T$$

$$\frac{1}{\tau_0} = k_F + k$$

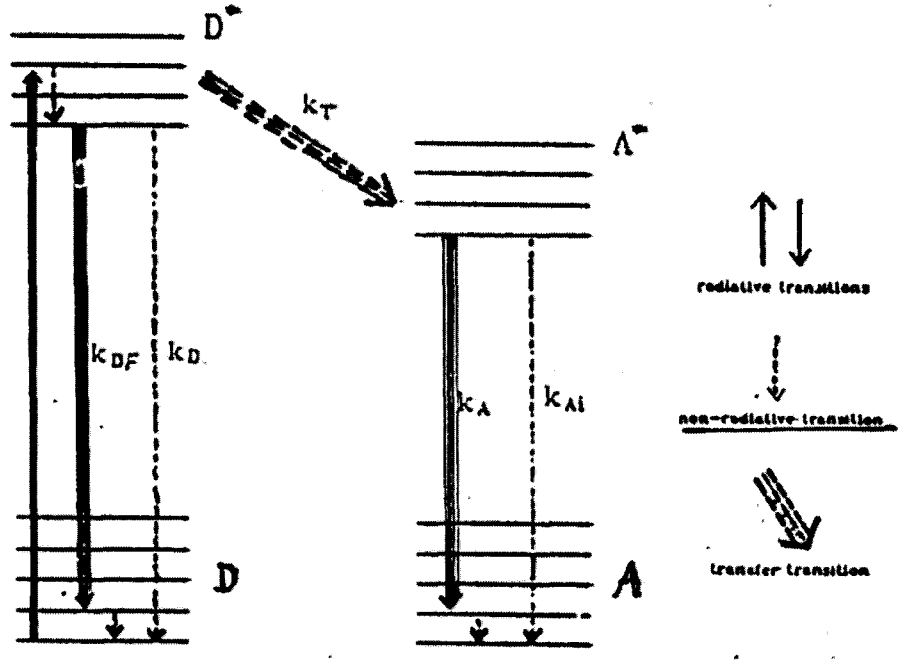

Simplified energy-level diagram of resonance energy transfer
D refers to the donor, and A to the acceptor; asterisks denote excited states. κ_D, κ_{fluo}, κ_T, $\kappa_{i,D}$ and κ_{Ai} are rate constants: κ_D and κ_{Df} for radiative and nonradiative deactivation of the excited donor state without transfer, κ_T for transfer, and κ_A and κ_{Ai} for radiative and nonradiative deactivation of the excited acceptor state without transfer.

$$E \equiv \frac{k_T}{k_T + k_F + k} = 1 - \frac{\tau}{\tau_0} = \frac{R_0^6}{R_0^6 + R^6}$$

normierte A-Fluoreszenzintensität

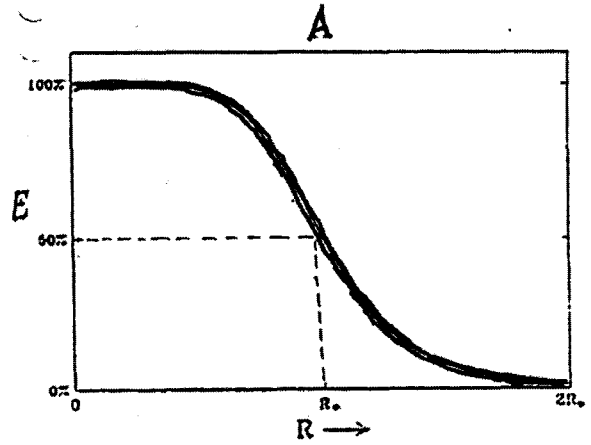

normierte D-Fluoreszenzintensität

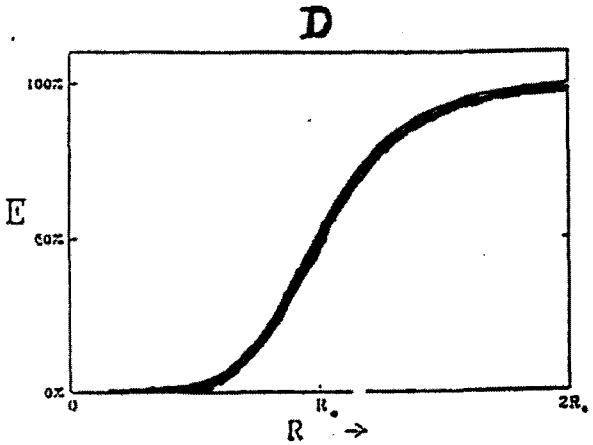

The transfer efficiency, E, versus the donor–acceptor distance, R (Å). Förster distance, R_0

7.2 FRET-Rate k_T

Donor-Bilanzgleichung

Anzahl der angeregten Donormoleküle N_D^*

$$\dot{N}_D^*(t) = -(k_F + k + k_T) N_D^*(t)$$

k_T = Transferrate D*A→DA*

$$N_D^*(t) = N_D^*(0)\, e^{-\frac{t}{\tau}}$$

τ_0 = F- Lebensdauer ohne Akzeptor

$$\frac{1}{\tau} = k_F + k + k_T = \frac{1}{\tau_0} + k_T$$

τ = F- Lebensdauer mit Akzeptor

$$\frac{\tau_0}{\tau} = 1 + \tau_0 k_T = \frac{F_0}{F}$$

F_0 = Fluoreszenzintensität des Donors ohne Akzeptor

F = Fluoreszenzintensität des Donors mit Akzeptor

$$E \equiv \frac{k_T}{k_T + k_F + k} = \frac{k_T \tau_0}{1 + k_T \tau_0} = 1 - \frac{F}{F_0} = \frac{1}{1 + \left(\frac{R}{R_0}\right)^6}$$

Transfer-Effizienz

Wenn jeder Donor mit einem Akzeptor im Abstand R benachbart ist, gilt für die in der Probe beobachtete Transferrate die Förster-Gleichung:

$$k_T = \frac{1}{\tau_0}\left(\frac{R_0}{R}\right)^6$$

Für $R = R_0$ ist $k_T = 1/\tau_0$ und $F_0/F = 2$, d. h.
die Hälfte des F-Lichts des D wird vom A absorbiert.

$$R_0^{\,6} = \frac{9 \ln 10 \kappa^2 Q_D J}{128 \pi^5 N_A n^4}$$

„Försterradius" R_0, wird aus Experimenten ohne Energietransfer bestimmt.

$$\kappa^2 = \left[\vec{e}_D \vec{e}_A - 3\vec{e}_D \vec{e}_R \circ \vec{e}_A \vec{e}_R\right]^2$$

Orientierungsfaktor der DDWW, Einheitsvektoren in Richtung des D-Emissions- und des A-Absorptionsdipols, sowie entlang des DA-Verbindungsvektors

$$Q_D = \frac{k_F}{k_F + k}$$

Quantenausbeute D-Fluoreszenz ohne Akzeptor

$$J = \int \lambda^4 \varepsilon_A(\lambda) f_D(\lambda) d\lambda$$

spektrales Überlappungsintegral

$\varepsilon_A(\lambda)$ Absorptionskoeffizient des Akzeptors (M^{-1} cm^{-1})

$f_D(\lambda)$ Normierte D-Fluoreszenzlinienfunktion ohne A

n Brechungsindex des Mediums zwischen D und A

Zur Begründung der Förster-Formel

(Quantenmechanische Herleitung der Förster-Formel siehe Praktikumsanleitung)

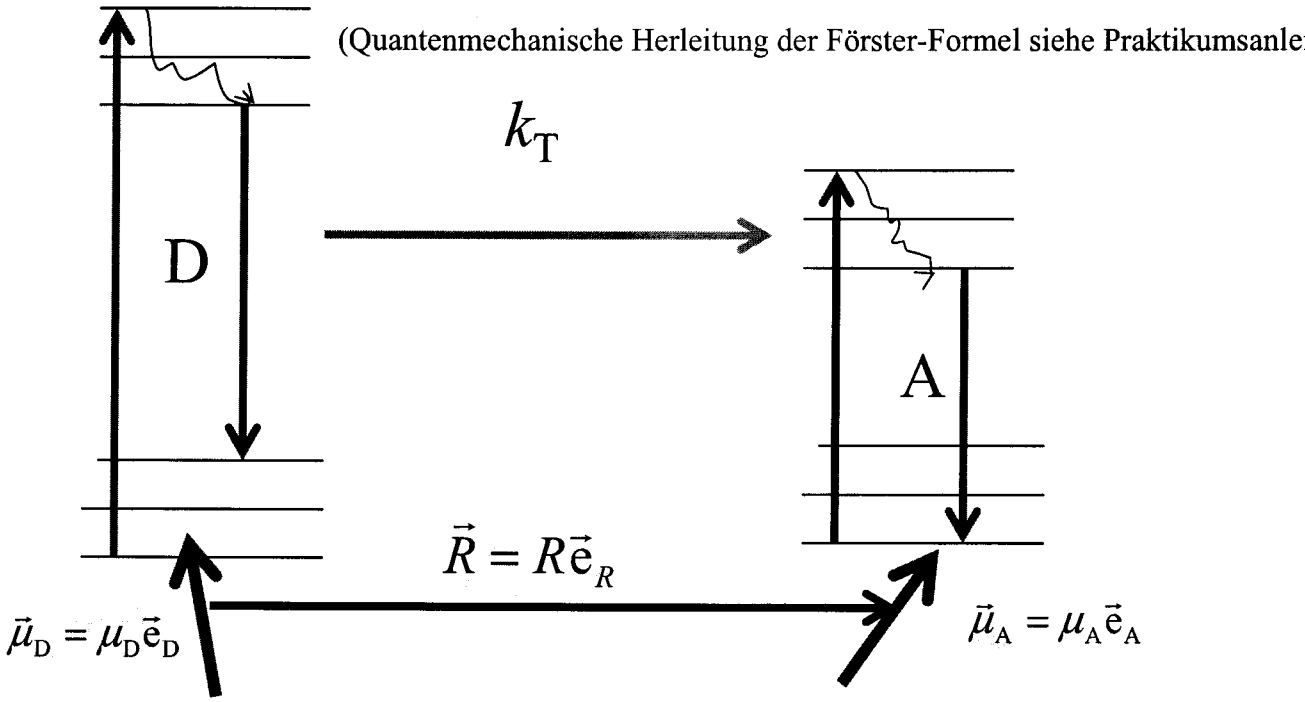

$$V(\vec{R}) = \frac{\kappa \mu_D \mu_A}{4\pi n^2 \varepsilon_0 R^3}$$

DDWW-Energie zwischen μ_D und μ_A

n = Brechungsindex des Lösemittels

$$\kappa \equiv \vec{e}_D \vec{e}_A - 3\vec{e}_D \vec{e}_R \circ \vec{e}_A \vec{e}_R$$ Richtungsfaktor $-2 \le \kappa \le 2$ (Größte Unsicherheit)

Wir nehmen zunächst an, dass der Donor nur bei der Winkelfrequenz ω emittiert, und zwar als Hertz'scher Dipol mit der Gesamtstrahlungsleistung

$$P_D(\omega) = \frac{2\mu_D{}^2 (1/2)\omega^4}{3 \cdot (4\pi n^2 \varepsilon_0) \cdot (c_0 / n)^3}$$

c_0 = Vakuumlichtgeschwindigkeit

Akzeptor-Absorptionsleistung bei ω

$$P_A(\omega) = \frac{1}{4} n^2 \varepsilon_0 \left(\frac{\kappa \mu_D}{R^3 4\pi n^2 \varepsilon_0} \right)^2 \cdot 3 \frac{c_0}{n} \varepsilon_A(\omega) \frac{\ln 10}{N_A}$$

kein H-Feld

Nah-E-Feld der D-Fluoreszenz

$\left\langle (\vec{e}_A \vec{e}_D)^2 \right\rangle = \frac{1}{3}$

A-Absorptionsquerschnitt

Bei der Definition des Absorptionsquerschnitts ist von isotroper Orientierung des Absorptionsdipols ausgegangen worden, hier ist die Orientierungsabhängigkeit im Faktor κ enthalten.

Für $R = R'_0$ wird die Hälfte der vom Donor emittierten Fluoreszenzstrahlungsleistung vom Akzeptor absorbiert:

$$P_A(\omega) = \frac{1}{2} P_D(\omega) \qquad \text{d. h.}$$

$$\frac{3}{4} \frac{n c_0 \varepsilon_0 \varepsilon_A(\omega) \ln 10}{N_A} \frac{\kappa^2 {\mu_D}^2}{{R'_0}^6 16\pi^2 {\varepsilon_0}^2 n^4} = \frac{1}{2} \frac{{\mu_D}^2 \omega^4 n}{3 \cdot 4\pi \varepsilon_0 {c_0}^3}$$

woraus mit $\omega = 2\pi\nu$ folgt $$R'_0{}^6 = \frac{9 \ln 10 \cdot \kappa^2 {c_0}^4}{128\pi^5 N_A n^4} \cdot \frac{\varepsilon_A(\nu)}{\nu^4}$$

Emittiert der Donor mit der Wahrscheinlichkeit $f_D(\nu)d\nu$ im Frequenzintervall ν... $\nu+d\nu$, dann ergibt sich für die sechste Potenz des modifizierten Försterradius der Ausdruck

$$R'_0{}^6 = \frac{9 \ln 10 \cdot \kappa^2 {c_0}^4}{128\pi^5 N_A n^4} \cdot \int f_D(\nu) \frac{\varepsilon_A(\nu)}{\nu^4} d\nu \qquad \frac{9 \ln 10}{128\pi^5 N_A} \approx 8{,}79 \cdot 10^{-28}\,\text{mol}$$

Mit $\frac{c_0}{\nu} = \lambda$ und $\int_0^\infty f_D(\nu) d\nu = \int_0^\infty f_D(\lambda) d\lambda = 1$ (Normierte D-Fluoreszenzfunktion bei Abwesenheit von A)

und Einbezug der D-Quantenausbeute (ohne A) in den modifizierten Förster-Radius ergibt sich für die Transferrate der gebräuchliche Ausdruck mit dem üblich als Försterradius bezeichneten Wert R_0

$$k_T = k_F \left(\frac{R'_0}{R}\right)^6 = \frac{Q_D}{\tau_0} \left(\frac{R'_0}{R}\right)^6 = \frac{1}{\tau_0} \left(\frac{R_0}{R}\right)^6$$

k_F ist die Emissionsrate von Fluoreszenzphotonen des Donors ohne Akzeptor

$Q_D = k_F/(k_F+k) = k_F\tau_0$ ist die Quantenausbeute des Donors ohne Akzeptor

Die aus der Förster-Transferrate folgende Abstandsabhängigkeit der Transfereffizienz mit der sechsten Potenz des D-A-Abstandes wurde an der unten abgebildeten Modellsubstanz demonstriert (*L. Stryer* et al. 1967)

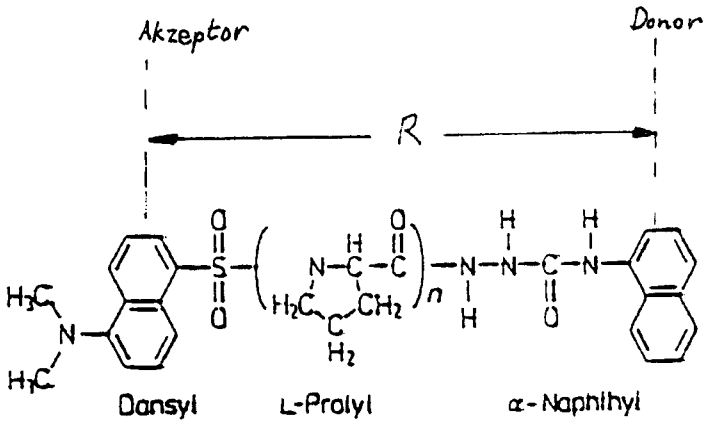

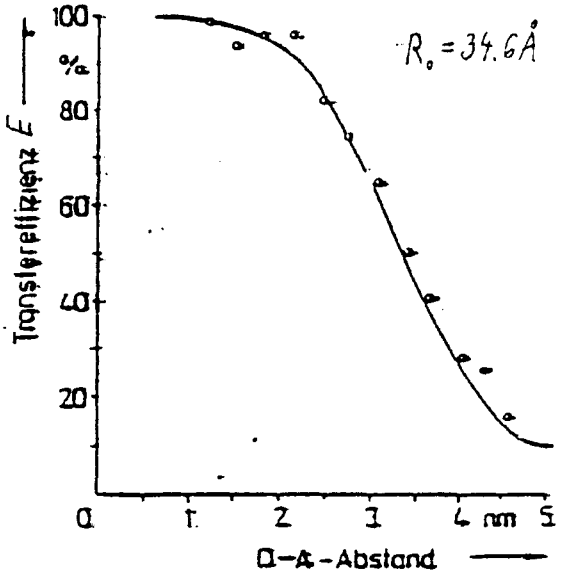

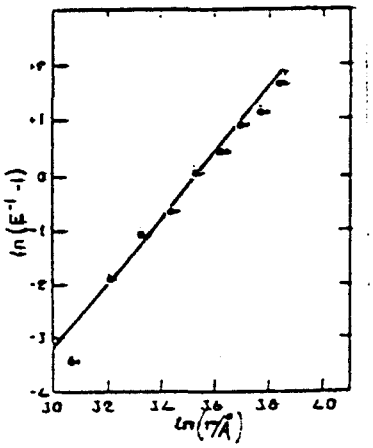

$$\ln\left(E^{-1}-1\right)=6\left[\ln R-\ln R_0\right]$$

$$E=1-\frac{\tau}{\tau_0} \qquad \tau_0 k_T=\left(\frac{R_0}{R}\right)^6 \qquad \frac{\tau_0}{\tau}=1+\left(\frac{R_0}{R}\right)^6$$

Die Überprüfung der R^6-Abhängigkeit war möglich, weil (L- prolyl)$_n$ eine konventionelle α-Helix mit bekannten Abständen ausbildet.

FRET in Einzelmolekülen

FRET-Messungen zwischen einem Donor und einem Akzeptor in einem Biomolekül (sp-FRET) kann Informationen über die Dynamik der Entfernungsfluktuationen zwischen der D- und der A-Region des Biomoleküls liefern.
Im Gegensatz zum Ensemble-FRET, bei dem nur Mittelwerte von Abständen ermittelt werden, kann man bei Einzelmolekül-FRET relativ direkt die Verteilung der Abstände und ihrer Dynamik bestimmen.

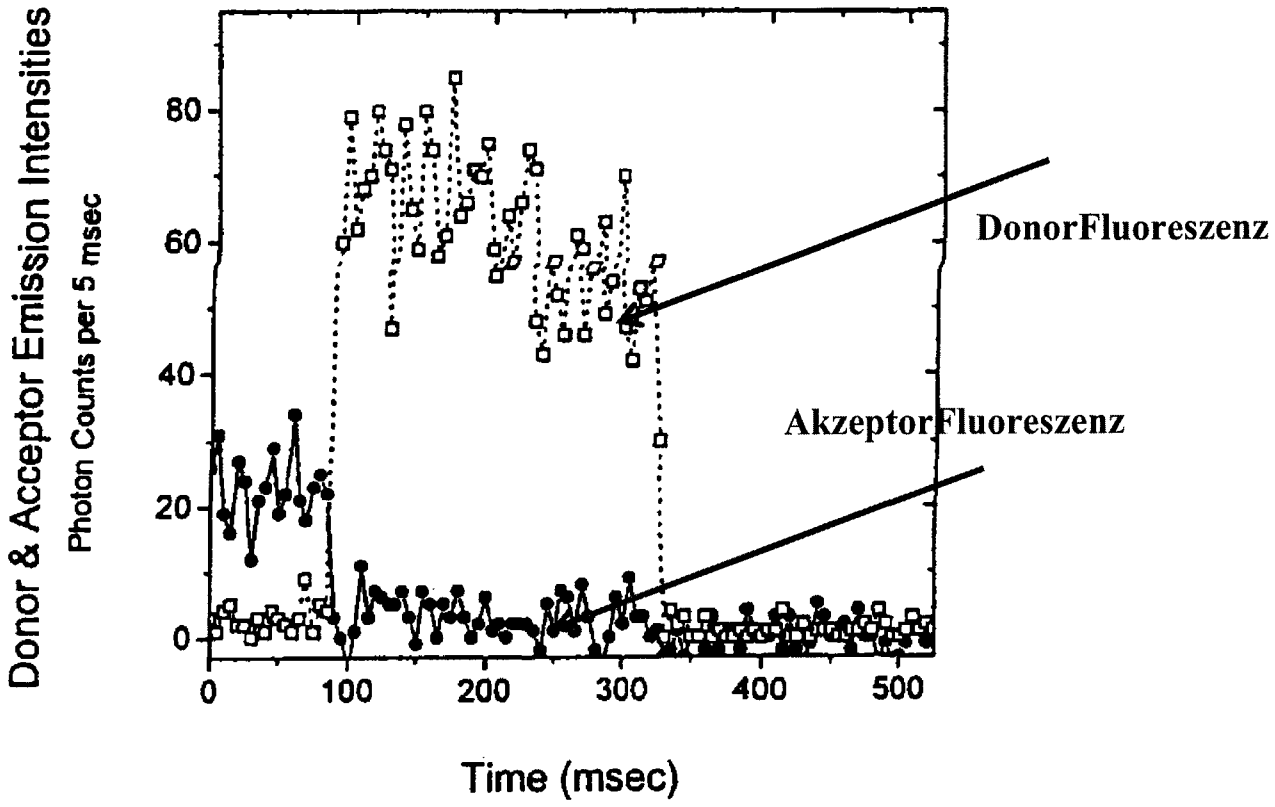

Die doppelt markierten Moleküle werden im Laserfokus positioniert (Einschränkung Fortbewegung z. B. durch Einbettung in Gel bzw. Oberflächenverankerung).

$$E(t) = \frac{1}{1+\gamma\frac{F_{\mathrm{D}}(t)}{F_{\mathrm{A}}(t)}}$$

Kalibrierungsfaktor γ

Anwendung von Mutanten des GFP (hier CFP und YFP) als Ca^{2+}-Sensor in Zellen (*Brasselet et al.* J. Phys. Chem. B104 3676 (2000).

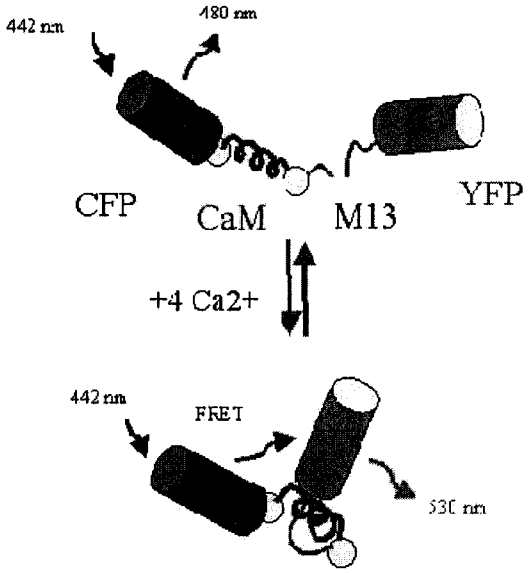

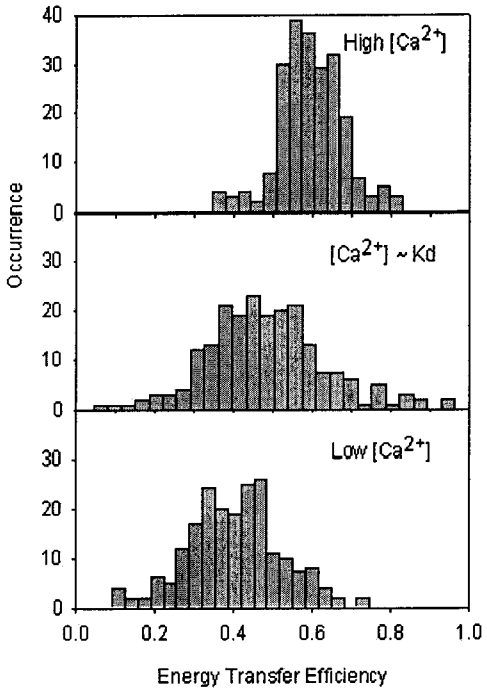

Das dunkelblau (cyan) fluoreszierende Protein CFP ist von dem gelb fluoreszierenden Protein YFP durch das Calmodulin /Ca2+ -Bindungsprotein CAM und ein Calmodulin-bindendes Peptid M13 getrennt. Bei der Bindung von Ca^{2+}-Ionen an den Komplex erfolgt eine Bindung des Calmodulins an M13 und diese Konformationsänderung bewirkt, dass der FRET CFP→YFP effektiver wird.
Dieser Komplex kann daher als Ca-Ionen Sensor in einer Zelle verwendet werden.

Die Einzelmolekül-FRET-Effektivität zeigt eine Verteilungsbreite, die bei der Gleichgewichtskonzentration am breitesten ist. Dies ist konsistent mit der Kinetik der Ligandenbindung, die in der Nähe des Gleichgewichts die größten Fluktuationen vorhersagt.

Die Integrationszeit bei den Messungen betrug 20 ms.

Die Reorientierung der F-Emissions- und F-Absorptionsdipole erfolgt schnell gegenüber der Integrationszeit, aber langsam im Vergleich zur Fluoreszenzlebensdauer.

Der resonante Fluoreszenztransfer CFP→YFP erfolgt in der 20 ms ...100 ms-Zeitskala.

Anwendungsbeispiel: FRET an Myosin, markiert mit BFP am C-Terminus und mit GFP am N-Terminus *Suzuki et al.* **Nature** 396 380 (1998)

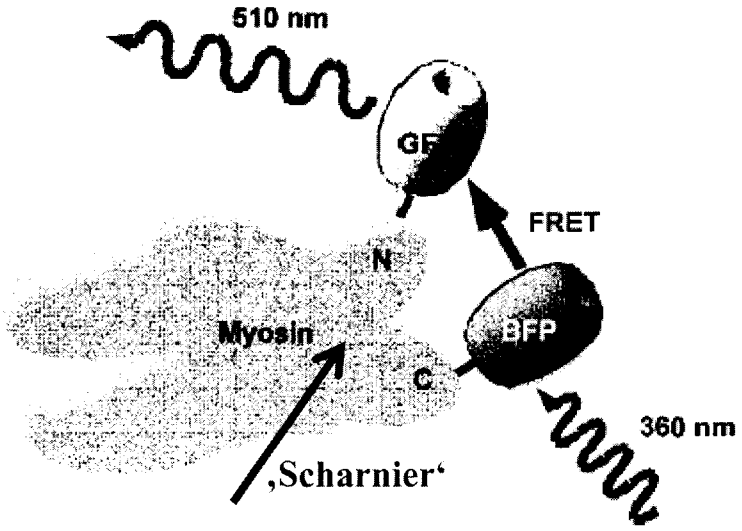

Motor-Protein Myosin: Der Abstand zwischen BFP und GFP verändert sich mit den Konformationsänderungen des Myosins bei ATP-Bindung und Hydrolyse im Einklang mit dem Hebel-Arm-Modell der Muskelkontraktion.

Zur Hebel-Arm-Hypothese

Huxley **Nature** 396 317 (1998)

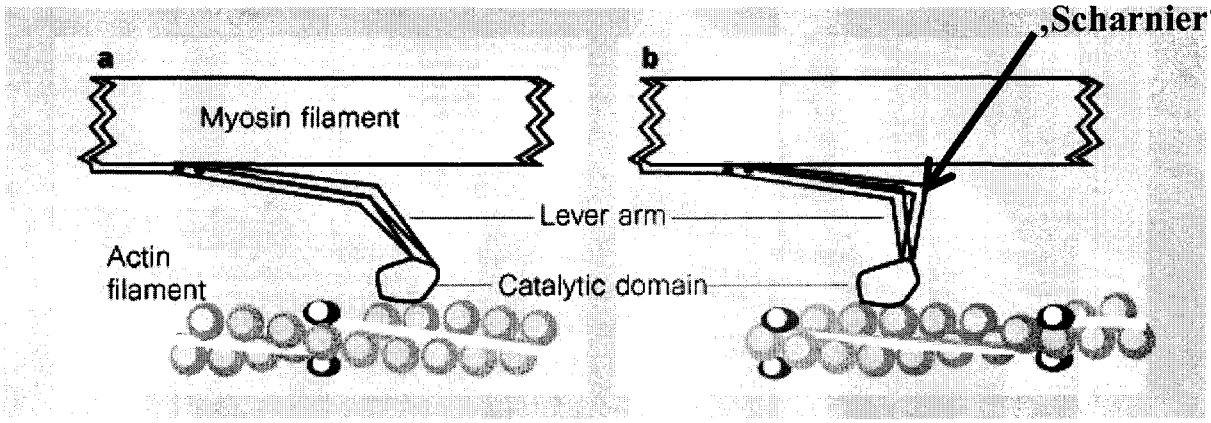

Figure 1 Presumed shape changes in a representative cross-bridge. a, During active contraction at fixed overall length; b, during rigor. Increase of length corresponds to displacement of the myosin filament to the left. The muscle is being subjected to a length oscillation with 3-nm peak-to-peak amplitude of relative sliding of filaments; the red outlines show the situation at the maximum length and the black outlines at the minimum. In a, the centre of mass of the lever arm is to the left of that of the catalytic domain, so that the contour of total mass of the cross-bridge is more spread out in the stretched case (red) than when shortened (black), respectively decreasing and increasing the intensity of the X-ray reflection corresponding to the repeat of myosin molecules along the filament. The intensity therefore fluctuates in opposite phase to the length. In b, the situation is reversed (centre of mass of the lever arm is to the right of that of the catalytic domain) and the intensity fluctuation is in phase with length.

Suzuki et al. benutzten ein Myosin-Fragment, das aus der katalytischen Domäne, dem angenommenen Scharnier und dem Anfang des daran beginnenden Hebelarms bestand.

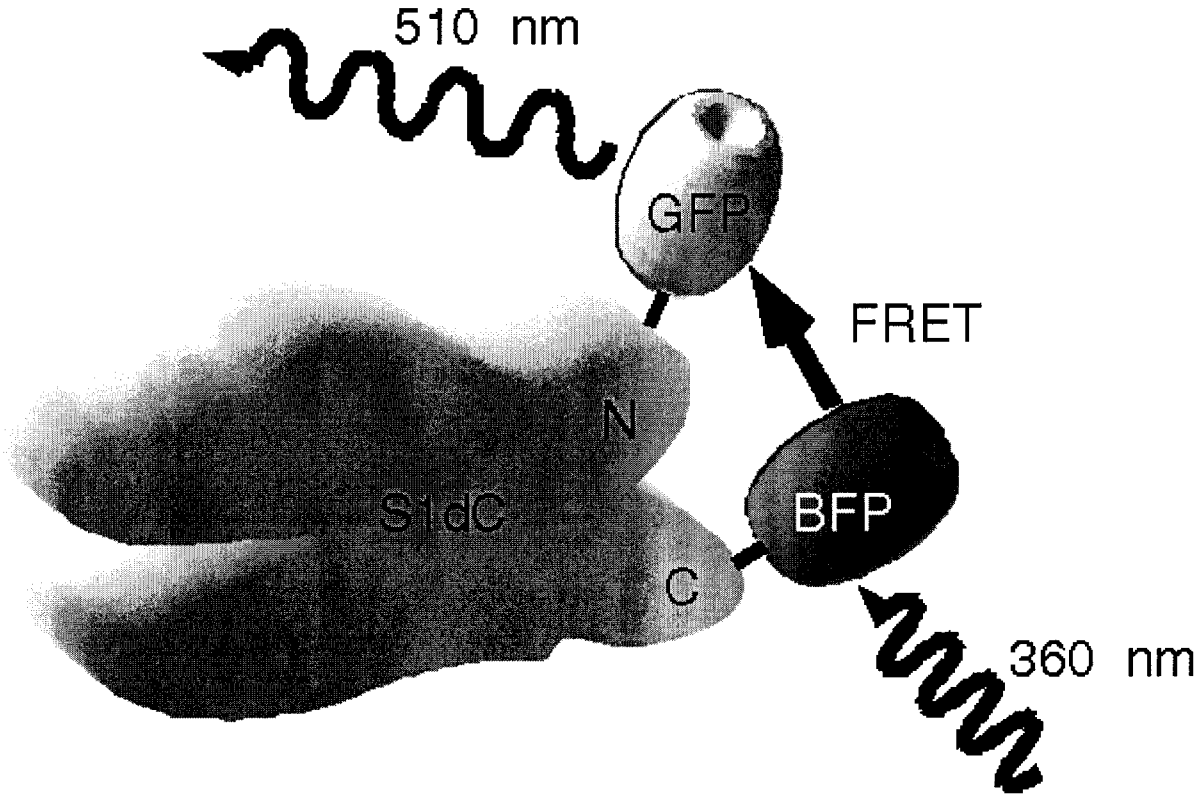

Figure 1 Diagrams of the domain of chimaeras made from the incorporation of fluorescent proteins into S1dC. **a**, The GFP, BFP and S1dC domains were connected by flexible spacers consisting of three glycine residues to generate GS1dCB and BS1dCG. **b**, When BFP was excited by light at 360 nm, intramolecular fluorescence resonance energy transfer (FRET) took place and green light was emitted at 510 nm from GFP. The intensity of the emission from GFP depended on the distance between GFP and BFP in the chimaeras.

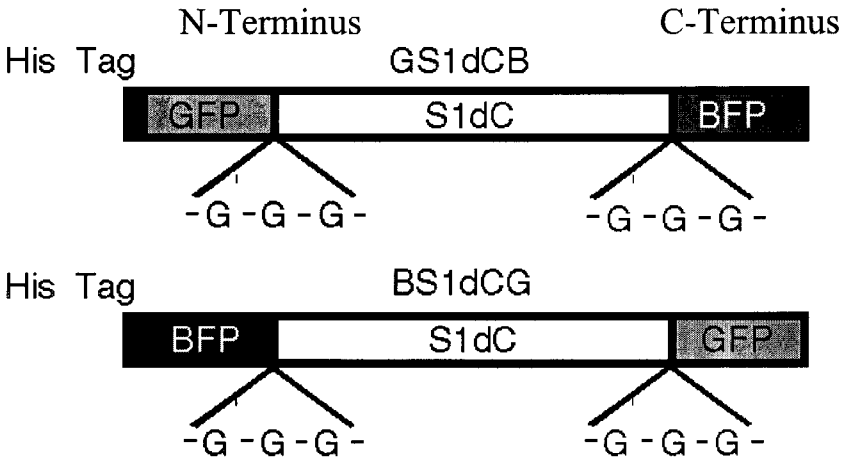

Suzuki et al. **Nature** 396 380 (1998)

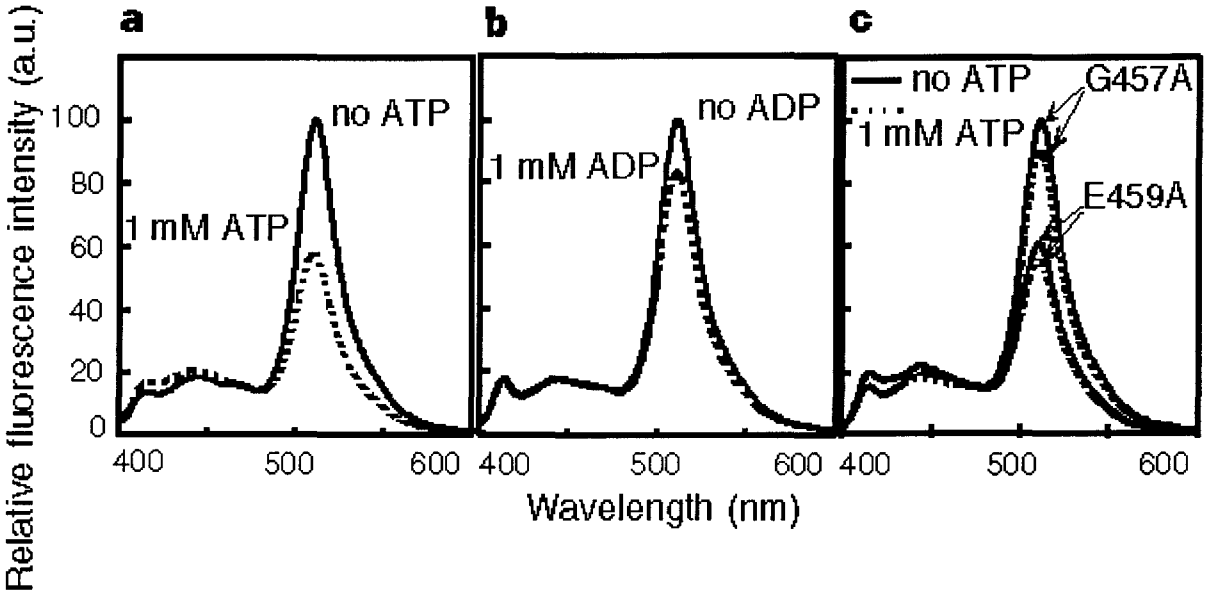

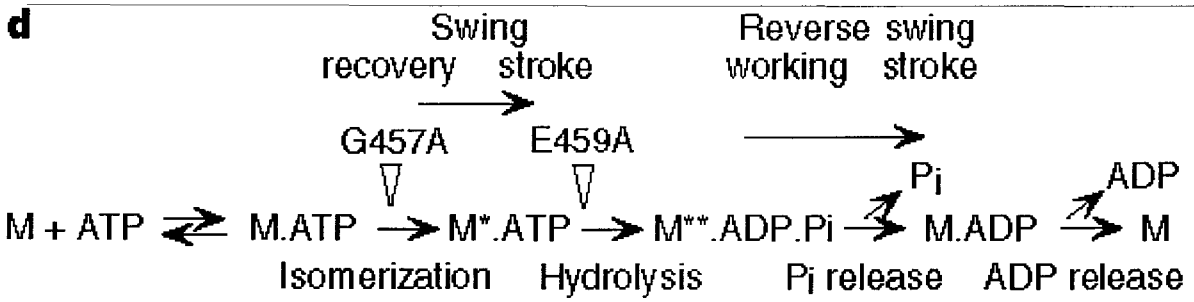

Figure 2 The relationship of FRET emission spectra in chimaeric S1dC to the hydrolysis of ATP. **a**, Emission spectra of GS1dCB excited at 360 nm in the presence and absence of ATP. **b**, Emission spectra of GS1dCB in the presence and absence of ADP. **c**, Emission spectra of G457A and E459A mutants of GS1dCB in the presence and absence of ATP. The spectra of the G457A mutant were similar to that of the wild-type chimaera without ATP, whereas those of the E459A mutant were similar to that of the wild-type with ATP. **d**, Intermediate states in the ATPase cycle of myosin[14,15]. M, M^* and M^{**} represent myosin in different conformational states as defined by their optical properties. Steps blocked by the G457A and E459A mutations are indicated by open arrowheads. The swing and reverse swing occur at the stages indicated.

$$E = \frac{F^{A}_{FRET}(510\,\mathrm{nm})}{F^{A}_{DIR}(510\,\mathrm{nm})} \cdot \frac{\varepsilon^{A}(480\,\mathrm{nm})}{\varepsilon^{D}(360\,\mathrm{nm})} - \frac{\varepsilon^{A}(360\,\mathrm{nm})}{\varepsilon^{D}(360\,\mathrm{nm})}$$

$$J = \int \lambda^4 f_D(\lambda)\varepsilon^{A}(\lambda)\mathrm{d}\lambda \approx 7{,}2 \cdot 10^{-14}\,\frac{\mathrm{cm}^3}{\mathrm{M}}$$

$$Q_D = 0{,}15$$

$$n = 1{,}4 \qquad \kappa^2 = \frac{2}{3}$$

Anwendungsbeispiel: FRET an Kinesin, modifiziert mit GFP beginnend bei Q339 und zusätzlichen Cys-Resten zur Markierung mit extrinsischen F-Sonden ***Rice et al.*** **Nature** 402 778, (1999)

a

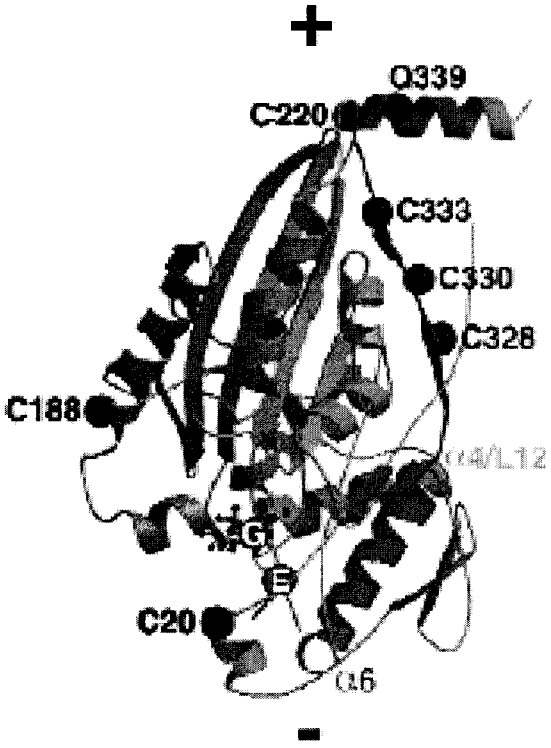

b

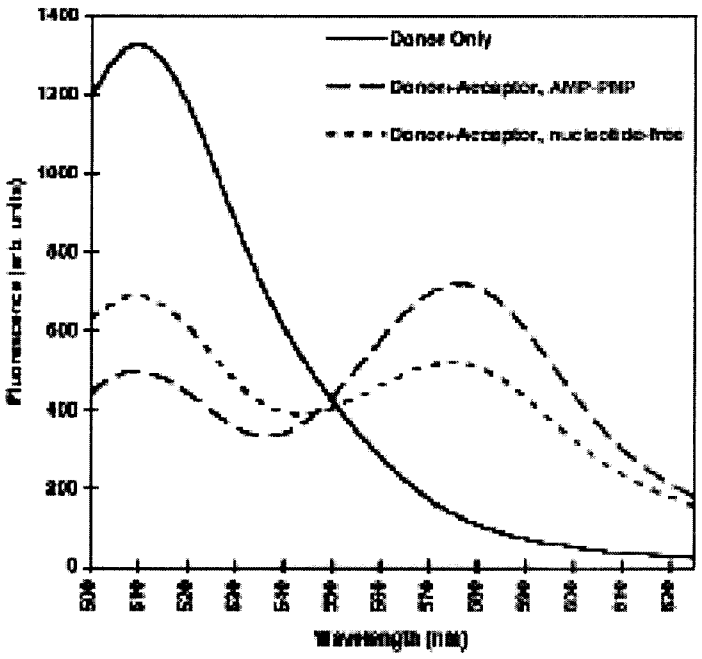

FRET von einem GFP-Donor bei Q339 zu einem Tetramethylrhodamin-Akzeptor bei C220. Die Donor-Fluoreszenz wird je nach Nukleotid-Anwesenheit unterschiedlich auf den Akzeptor übertragen. Die Messung des FRET in unterschiedlichen Nukleotid- und Mikrotubul-Bindungszuständen erlaubt die Ableitung eines strukturellen Modells für die Bewegung des Kinesins entlang eines Mikrotubuls.

acceptor. You should be able to show that

$$\tau_{D,A}/\tau_D = 1 - E \tag{8-53}$$

Measurement of energy transfer by direct observation of lifetimes is quite important because it avoids a potential trivial effect that can mimic transfer.

A requirement for the resonance interaction producing energy transfer is that acceptor absorption must overlap the donor fluorescence (Fig. 8-18). Therefore, in any system capable of energy transfer, an additional process may occur in which the donor emits a photon that is then reabsorbed by the acceptor. This is distinguishable from true singlet–singlet energy transfer, because it leaves the rate of donor emission unchanged. Trivial emission and reabsorption of photons can be detected by comparing the efficiencies derived from Equations 8-53 and 8-49 or 8-52. It can be avoided by working at total chromophore concentrations less than about 10^{-3} M.

Measuring interchromophore distances from energy-transfer efficiencies

To obtain useful structural information from energy transfer, the measured efficiency must be related to the distance R between the two chromophores. This can be done by using the theory developed by Theodore Förster. He computed that the rate of transfer is

$$k_T = (1/\tau_D)(R_0/R)^{-6} \tag{8-54}$$

where τ_D is the lifetime of the donor in the absence of the acceptor. The inverse sixth power comes from the square of the dipole–dipole coupling, which depends on R^{-3} (see Box 8-3). R_0 is called the characteristic transfer distance:

$$R_0 = 9.7 \times 10^3 (J\kappa^2 n^{-4} \phi_D)^{1/6} \text{ cm} \tag{8-55}$$

where

$$J = \int \varepsilon_A(\nu) f_D(\nu) \nu^{-4} \, d\nu \tag{8-56}$$

J is a measure of the spectral overlap between donor emission and acceptor absorption (shaded in Fig. 8-18); f_D is the normalized fluorescence of the donor as defined in Equation 8-42; n is the refractive index of the medium between donor and acceptor; ϕ_D is the quantum yield of donor in the absence of the acceptor; and κ^2 is a complex geometric factor that depends on the orientation of donor and acceptor. If both donor and acceptor are free to tumble rapidly on the time scale of fluorescence emission, κ^2 approaches a limiting value of 2/3. (The origins of all these quantities in Eqns. 8-54, 8-55, and 8-56 are described in Box 8-3.)

Box 8-3 THE FÖRSTER THEORY OF SINGLET–SINGLET ENERGY TRANSFER

Here we sketch an oversimplified derivation of Equations 8-54, 8-55, and 8-56. We start with Equation 7-27, which says that the rate of exciting a molecule is proportional to the square of the expectation value of the interaction causing the excitation. Although we derived this equation for a particular case, it turns out to be a very general result, often called Fermi's Golden Rule. We want to compute the rate at which the state of the chromophore pair D and A changes from $\Psi_{D_b}\Psi_{A_a}$ to $\Psi_{D_a}\Psi_{A_b}$.

We first consider the case where the $a \leftrightarrow b$ transitions of both D and A occur at the same frequency, ν. To describe the weak interaction between D and A, we use the same dipole–dipole coupling described earlier for the somewhat stronger interactions that produce exciton splitting. Therefore, the rate of energy transfer should be proportional to the following expression:

$$k_T(\nu) \propto |\langle \Psi_{D_a}\Psi_{A_b}|\underset{\sim}{V}|\Psi_{D_b}\Psi_{A_a}\rangle|^2$$

where $\underset{\sim}{V}$ is given (by analogy to Eqn. 7-48) as

$$\underset{\sim}{V} = (\underset{\sim}{\mu}_D \cdot \underset{\sim}{\mu}_A)/R^3 - 3(\underset{\sim}{\mu}_D \cdot \mathbf{R})(\mathbf{R} \cdot \underset{\sim}{\mu}_A)/R^5$$

where $\mathbf{R}$ is the distance between donor and acceptor, and $\underset{\sim}{\mu}_D$ and $\underset{\sim}{\mu}_A$ are dipole moment operators.

If all effects of the orientation of D and A are lumped into a parameter κ, then we can rewrite $\underset{\sim}{V}$ as

$$\underset{\sim}{V} = \kappa|\underset{\sim}{\mu}_D||\underset{\sim}{\mu}_A|/R^3$$

where the vertical bars indicate that only the lengths of $\underset{\sim}{\mu}_D$ and $\underset{\sim}{\mu}_A$ must be evaluated. Substitution of this expression for $\underset{\sim}{V}$ into the earlier equation for the transfer rate, k_T, yields

$$k_T(\nu) \propto |(\kappa/R^3)\langle \Psi_{D_a}\Psi_{A_b}||\underset{\sim}{\mu}_D||\underset{\sim}{\mu}_A||\Psi_{D_b}\Psi_{A_a}\rangle|^2$$

Because $\underset{\sim}{\mu}_D$ depends only on the electronic coordinates of the donor group, and $\underset{\sim}{\mu}_A$ depends only on the acceptor group, this expression can be factored to give

$$k_T(\nu) \propto (\kappa^2/R^6)|\langle \Psi_{D_a}|\underset{\sim}{\mu}_D|\Psi_{D_b}\rangle|^2|\langle \Psi_{A_b}|\underset{\sim}{\mu}_A|\Psi_{A_a}\rangle|^2$$

You can see that the transfer rate will depend on the inverse sixth power of the distance. The term in $\underset{\sim}{\mu}_A$ is just the dipole strength of the acceptor, which in turn can be related to an integral over the absorption spectrum using Equation 7-40. In the case we are considering, absorption takes place only at a single frequency ν, and so Equation 7-40 becomes

$$|\langle \Psi_{A_b}|\underset{\sim}{\mu}_A|\Psi_{A_a}\rangle|^2 \propto \varepsilon_A \nu^{-1}$$

The term in $\underset{\sim}{\mu}_D$ is the dipole strength of the donor, which can be related to the fluorescence rate.

Using Equations 8-32 and 8-34, we have

$$D_{ab} \propto \nu^{-3} A_{ba} = \nu^{-3} \tau_R^{-1}$$

From Equation 8-41, we can replace τ_R^{-1} by ϕ_D/τ_D, where ϕ_D is the quantum yield of the donor, and τ_D is the lifetime of the donor in the absence of the acceptor. Then

$$|\langle \Psi_{D_a} | \underset{\sim}{\mu}_D | \Psi_{D_b} \rangle|^2 \propto \nu^{-3} \phi_D/\tau_D$$

Using all these results, we can write the energy transfer rate as

$$k_T(\nu) \propto (\kappa^2/R^6)(\phi_D/\tau_D)\varepsilon_A \nu^{-4}$$

Now we consider the general case where the acceptor absorption occurs over a band of frequencies, so that ε_A is a function of ν. Similarly, the fluorescence of the donor occurs over a range of frequencies. Let $f_D(\nu)$ be the fraction of donor fluorescence at frequency ν. The total rate of energy transfer can be computed by integrating the rate expected at each frequency:

$$k_T \propto (\kappa^2/R^6)(\phi_D/\tau_D) \int \varepsilon_A(\nu) f_D(\nu) \nu^{-4} d\nu = (\kappa^2 \phi_D/R^6 \tau_D) J$$

This expression is identical to Equations 8-54, 8-55, and 8-56, except for numerical constants and the appearance of n, the refractive index. The presence of n comes from the fact that $\underset{\sim}{V}$ as written above applies only in vacuum; in a fluid medium, the true interaction potential at optical frequencies is $\underset{\sim}{V}/n^2$.

The troublesome part of the Förster theory is the inclusion of the quantity κ^2. Removing the orientation dependence of the donor and acceptor interaction (as we did above) implies that orientations are sampled rapidly during the time the donor is excited. This may not always be true. Unfortunately, κ^2 cannot be measured directly. From the definition of $\underset{\sim}{V}$, we know that κ^2 must have a value between 0 and 4. Measurements of fluorescence polarization can place narrower limits on κ^2 in each particular case. Uncertainties in the κ^2 value still are a major source of error in distance determinations using energy transfer. Fortunately, the distance R will depend only on $(\kappa^2)^{1/6}$, as you can see by rewriting Equation 8-57 in this form:

$$R = R_0[(1 - E)/E]^{1/6}$$

In actuality, using Equations 8-55 and 8-56, it is more convenient to use spectra measured on a wavelength scale and to express the result in angstroms. Then Equations 8-55 and 8-56 become

$$R_0 = 8.79 \times 10^{-5} (J \kappa^2 n^{-4} \phi_D)^{1/6} \text{ Å}$$

$$J = \int \varepsilon_A(\lambda) f_D(\lambda) \lambda^4 d\lambda$$

The efficiency of energy transfer can be calculated by rewriting Equation 8-48 as $E = k_T/(k_T + 1/\tau_D)$. Then, substitution of Equation 8-54 for k_T yields

$$E = R_0^6/(R_0^6 + R^6) \tag{8-57}$$

The result is plotted as the solid line in Figure 8-20 for a particular value of R_0. It is apparent that, for distances near R_0, a measurement of E can yield a fairly accurate determination of the distance. For commonly used pairs of chromophores, R_0 varies from 10 Å to more than 50 Å. Therefore, distances up to about 80 Å are measurable.

The most critical test of the Förster theory came from the work of Lubert Stryer and Richard Haugland (1967). They prepared a set of terminally labeled oligopeptides:

Dansyl—$(Pro)_n$—NH—NH—CO—NH—Naphthyl

The proline residues formed a polyproline type-II helix, which could be confirmed by CD measurements. Because the distance between naphthyl donor and dansyl acceptor was known from the known dimensions of the helix, measured efficiencies could be compared directly with computed values from the Förster theory; the agreement is excellent (Fig. 8-20). Since this pioneering work, energy transfer has been used to measure distances within tRNA, immunoglobulins, rhodopsin, and oligopeptides, and between the protein subunits of assemblies ranging from simple oligomeric proteins to ribosomes. The most difficult part of these measurements is the specific introduction of the two fluorescent chromophores into known portions of the structures. For the full spectrum of measurements, three replica systems must be prepared. They should be as identical as possible, except that one has only donor, one has donor and acceptor, and one has only acceptor.

Energy transfer plays a large role in determining the emission spectrum of normal proteins. The fluorescence of tyrosine is overlapped by the absorption of tryptophan. Although the R_0 for this donor-acceptor pair is only ~ 9 Å, it is still appreciable compared with average distances expected for tyrosine–tryptophan nearest-neighbor pairs in a globular protein.[§] The result is that the tyrosines are extensively quenched; almost all of the observed emission comes from tryptophan (as we mentioned earlier).

Fluorescence polarization

If plane-polarized light is used to excite a fluorescent system, and if linearly polarized components of the emission are detected, information can be obtained about the size, shape and flexibility of macromolecules. Figure 8-21 shows a typical experimental

[§] A spherical protein of 17,000 mol wt will have a radius (r) of about 17 Å. The root-mean-square distance between random selected pairs of points within a spherical volume is $\sqrt{6/5}\, r$. So even a single tryptophan in such a protein is likely to be near enough to many tyrosines to cause appreciable energy transfer.

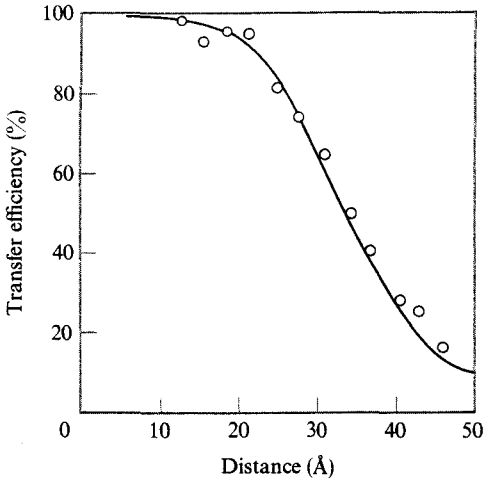

Figure 8-20

Efficiency of energy transfer as a function of distance in dansyl-(L-prolyl)$_n$-α-naphthyl semicarbazide oligomers with $n = 1$ to 12. The curve was fit to the data with Equation 8-57. [From L. Stryer and R. P. Haugland, *Proc. Natl. Acad. Sci. USA* 98:719 (1967).]

arrangement. Light is incident along the x axis and is detected along the y axis. The incident light is polarized along the z axis. Two components of the emitted light are measured: $I_{||}$ is polarized along the z axis, and $I_{\perp}$ is polarized along the x axis. There can be no emission propagating along the y axis that is also polarized along this axis because light, like all electromagnetic radiation, is a transverse wave.

Polarization of rigid systems

First, consider a rigid, isotropic sample. This sample could correspond to a frozen solution of fluorescent molecules, or to chromophores on randomly oriented molecules so large that no appreciable molecular rotations occur on the fluorescence time scale (typically < 100 nsec). The vector $\boldsymbol{\mu}$ defines the orientation of the absorption transition dipole moment ($\langle \Psi_b | \tilde{\boldsymbol{\mu}} | \Psi_a \rangle$) of one chromophore relative to the laboratory coordinates. The probability that this chromophore will be excited is proportional to $(\tilde{\boldsymbol{\mu}} \cdot \mathbf{E})^2$. Because $\mathbf{E}$ is parallel to the z axis, this probability is $\cos^2 \theta$, where θ is the angle between $\boldsymbol{\mu}$ and the z axis. Therefore, molecules oriented with transition dipoles near the z axis will be preferentially excited. This is the principle called *photoselection.*

To explain fluorescence polarization, we need to calculate the probability of exciting molecules with particular orientations. Then we must compute the probability that these molecules will emit light polarized in certain directions. It is convenient to use spherical polar coordinates (Fig. 8-21). Before excitation, the relative number of molecules with μ oriented at angles between θ to $\theta + d\theta$ and ϕ to $\phi + d\phi$ is $\sin \theta \, d\theta \, d\phi$. (The factor of $\sin \theta$ enters because it is much more probable to find molecules perpendicular to the z axis than parallel to it.) The probability of exciting a molecule oriented at θ and ϕ is proportional to $\cos^2 \theta$, as mentioned earlier. Therefore, the

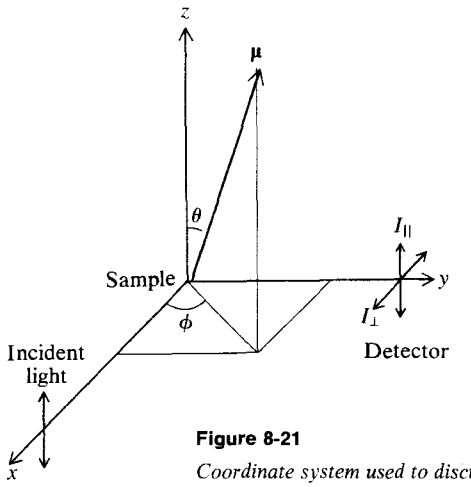

Figure 8-21
Coordinate system used to discuss fluorescence polarization.

relative number of excited molecules oriented at θ to $\theta + d\theta$ and ϕ to $\phi + d\phi$ is

$$P(\theta, \phi)\, d\theta\, d\phi \propto \cos^2 \theta \sin \theta\, d\theta\, d\phi \tag{8-58}$$

The fraction of excited molecules oriented at θ to $\theta + d\theta$ and ϕ to $\phi + d\phi$ is

$$W(\theta, \phi)\, d\theta\, d\phi = P(\theta, \phi)\, d\theta\, d\phi \Big/ \int_0^{\pi} d\theta \int_0^{2\pi} d\phi \cos^2 \theta \sin \theta\, d\theta\, d\phi \tag{8-59}$$

The integral in Equation 8-59 simply counts all excited molecules. It can be performed by substituting $x = \cos \theta, dx = -\sin \theta$, and so on. The result is $4\pi/3$, so Equation 8-59 becomes

$$W(\theta, \phi)\, d\theta\, d\phi = (3/4\pi) \cos^2 \theta \sin \theta\, d\theta\, d\phi \tag{8-60}$$

Note that this result depends only on θ. The distribution of excited molecules is cylindrically symmetric about the z axis. (Fig. 8-22 shows a plot of Eqn. 8-60.) Note that excited molecules have transition dipoles oriented preferentially toward the z axis and not along the x axis.

Because the distribution of excited molecules is anisotropic, the resulting fluorescence also will be anisotropic. To calculate this, we must know the relative directions of absorbing and emitting transition dipoles in the chromophore. If the same electronic transition that absorbed does the emitting ($S_a \rightarrow S_b$ followed by $S_b \rightarrow S_a$), then emitting and absorbing transition dipoles are parallel. The probability that emission will occur polarized along the z axis is proportional to $|\boldsymbol{\mu} \cdot \hat{\mathbf{k}}|^2$, where $\hat{\mathbf{k}}$ is a unit vector along the z axis. This expression is proportional to $\cos^2 \theta$. To find the relative emission intensity polarized along z, we must multiply the probability

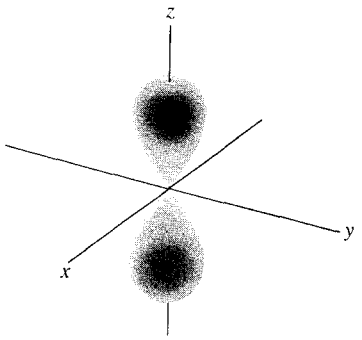

Figure 8-22

Distribution of excited chromophores produced by exciting a sample with z-polarized light propagating along the x axis. The density of the shading is proportional to the probability of finding an excited molecule with its transition dipole at that particular orientation.

of emission by the fraction of excited molecules with each orientation, $W(\theta, \phi)$, and average over all orientations:

$$I_{||} \propto \int_0^{2\pi} d\phi \int_0^{\pi} d\theta \cos^2 \theta \, W(\theta, \phi) = (3/4)\pi \int_0^{2\pi} d\phi \int_0^{\pi} d\theta \cos^4 \theta \sin \theta = 3/5 \quad (8\text{-}61)$$

The probability of emission polarized along the x axis is proportional to $|\boldsymbol{\mu} \cdot \hat{\mathbf{i}}|^2$, where $\hat{\mathbf{i}}$ is a unit vector along x. This expression is proportional to $(\sin \theta \cos \phi)^2$. To calculate the relative emission intensity, $I_\perp$, we again average emission probabilities over the distribution of excited molecules:

$$I_\perp \propto \int_0^{2\pi} d\phi \int_0^{\pi} d\theta \sin^2 \theta \cos^2 \phi \, W(\theta, \phi) = (3/4)\pi \int_0^{2\pi} d\phi \cos^2 \phi \int_0^{\pi} d\theta \cos^2 \theta \sin^3 \theta = 1/5 \quad (8\text{-}62)$$

In practice, what is done is to measure $I_{||}$ and $I_\perp$ and compare. Two convenient comparisons of $I_{||}$ and $I_\perp$—the polarization (P) and the anisotropy (A)—are defined in Equation 8-63 (see also Box 8-4).

$$P = (I_{||} - I_\perp)/(I_{||} + I_\perp) \qquad A = (I_{||} - I_\perp)/(I_{||} + 2I_\perp) \quad (8\text{-}63)$$

For the totally rigid system we have just described, $P = 1/2$ and $A = 2/5$, as you can see by substituting the results of Equations 8-61 and 8-62 into Equation 8-63. These turn out to be the maximal values of polarization and anisotropy possible under any circumstances.

Box 8-4 POLARIZATION AND ANISOTROPY

The definitions of polarization and anisotropy are not as arbitrary as they seem. P is defined by analogy with the dichroic ratio described in Equation 7-42. It is a relatively simple quantity to measure directly. A is more useful for analysis of experimental data on complex systems. The denominator of A is simply the total light that would be observed if no polarizers were used (see figure). Nonpolarized light incident along x can be resolved into y- and z-polarized

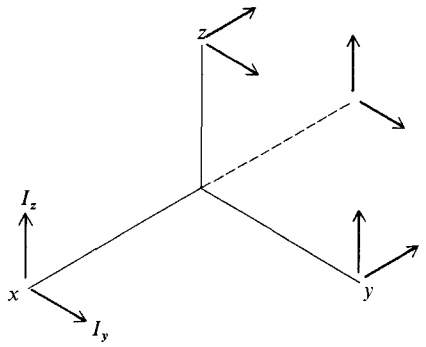

components. The total emission can be found by adding emission along all three Cartesian axes. For z-polarized excitation, there are two perpendicular components propagating along z, and one parallel and one perpendicular component, each propagating along x and y. For y-polarized excitation, there are two perpendicular components propagating along y, and one parallel and one perpendicular component, each propagating along x and z. The result is $8I_{\perp}$ plus $4I_{\parallel}$. Therefore, the total emission has twice as much perpendicular component as parallel component.

Anisotropy has a substantial advantage in many applications because various equations using it are simpler than the corresponding equations for polarization. Another advantage comes in the analysis of mixtures. Multicomponent mixtures of substances with equal fluorescence intensity but variable anisotropy (A_i) show a total anisotropy equal to $\sum_i \chi_i A_i$, where χ_i is the mole fraction of the ith component. Polarization does not obey such simple relationships. However, polarization and anisotropy can be interconverted by the relationship

$$[(1/P) - (1/3)]^{-1} = 3A/2$$

which you should be able to derive from Equation 8-63.

Another common case is a system in which the emission transition dipole is perpendicular to the absorption transition dipole. This will occur in many planar chromophores if absorption takes place into the second excited singlet state, but emission is observed from the first excited singlet. In this case, still for a rigid system, $P = -1/3$ and $A = -1/5$. See if you can derive these values by calculating averages analogous to those worked out for the case just discussed.

The polarization or anisotropy for a rigid system is called the limiting value, and it is denoted by subscript zero. In general, it is given by

$$P_0 = (3\cos^2\xi - 1)/(\cos^2\xi + 3) \qquad A_0 = (3\cos^2\xi - 1)/5 \tag{8-64}$$

where ξ is the angle between absorption and emission transition dipoles. These expressions provide a method of measuring ξ in rigid systems.

Now consider the other extreme case, in which (during the lifetime of the excited state) the chromophore can tumble fast enough to randomize its orientation. In this case, by the time emission occurs, all memory of the original photoselection is lost. Thus $I_{||} = I_{\perp}$, and the polarization and anisotropy are both zero.

● Effect of molecular motion

Most macromolecules of biological interest fall between the two extreme cases just described: their rotational motions are *not* negligible on the fluorescence time scale, but neither can they tumble fast enough to achieve random orientation. Suppose that a fluorescent probe is rigidly attached to the macromolecule. The observed polarization will be some intermediate value between Equation 8-64 and zero. To compute this value, we must analyze the relative rates of emission and macromolecular rotational motion. Note that translational motion does not affect fluorescence polarization. Only motion that changes the *orientation* of the transition dipoles can be observed.

First consider what happens if the sample is excited by a pulse of polarized light, and the time dependence of $I_{||}$ and $I_{\perp}$ is measured. If emission and absorption dipoles are parallel, the earliest photons to be emitted are highly likely to be z-polarized because the molecules have not had time to reorient. The last photons to be emitted should have random polarization because by then the system has experienced considerable rotational motion. Therefore, if the polarization or anistropy is measured as a function of the time of fluorescence emission, it will decay from initial values of P_0 or A_0 to final values of zero. The rate of decay is a measure of the rate of rotational motion.

Rotational Brownian motion is described by a diffusion equation quite analogous